MUON-COMPUTED TOMOGRAPHY USING POCA TRAJECTOY FOR IMAGING SPENT NUCLEAR FUEL IN DRY STORAGE CASKS

Zhengzhi Liu[*†], Stylianos Chatzidakis[*], John M. Scaglione[*], Can Liao[††], Haori Yang[††], and Jason P. Hayward[*†]

[*]*Oak Ridge National Laboratory, Oak Ridge, TN 37831*
[†]*Department of Nuclear Engineering, University of Tennessee, Knoxville, TN 37996*
[††]*School of Nuclear Science and Engineering, Oregon State University, Corvallis, OR 97331*
zliu36@vols.utk.edu

Cosmic ray muon-computed tomography (μCT) is a new imaging modality with unique characteristics that can be particularly important for applications in nuclear proliferation detection and international treaty verification. Using cosmic ray muons for nuclear security presents several potential advantages. Among others, muons are generated naturally in the atmosphere, can penetrate high-density materials, and are freely available. No radiological sources are required and consequently there is no associated radiological dose. Recently, the feasibility of using muons for imaging spent nuclear fuel stored in shielded casks has been explored and has been proved beneficial. However, challenges in μCT imaging include low muon flux of ~10,000 muons/m^2/min, the effects of multiple Coulomb scattering (MCS) blurring the image, and inefficiency in being able to use all recorded muons for imaging. In this paper, we argue that the use of muon tracing should produce tomographic muon images with improved quality – or more quickly for the same image quality – compared to the case where conventional methods are used. In our paper, we report on the development and assessment of a novel muon tracing method for μCT. The proposed method back projects the muon's scattering angle into each pixel crossed by its PoCA trajectory then forward projects the variance of the scattering angle in each pixel to detector bins along the muon's incident horizontal direction. Two scenarios were simulated to assess the expected detection capability of this proposed method. GEANT4 was used to model the main characteristics of 1-60 GeV muons through matter. The simulated images showed an expected improvement in resolution and a reduced the reliance on the muon momentum information compared to a more conventional muon tomography method.

INTRODUCTION

Cosmic ray muon-computed tomography (μCT) has several potential advantages in proliferation detection and international treaty verification [1]. The passive nature of cosmic ray muons, very high energies on the order of GeV, high penetrating ability, and unique image formation characteristics can reconstruct heavily shielded objects [2-4]. An additional potential advantage in recent μCT applications is the availability of detectors that measure the positions and directions of the individual muons before and after traversing the object under investigation [5-8]. An application of interest in which μCT can prove beneficial is imaging of spent nuclear fuel stored in shielded dry casks [9-16]. Monitoring nuclear waste and having an ability to understand if there have been changes to the spent nuclear fuel geometry after transportation are important for waste management system planning efforts. However, challenges in μCT include low muon flux, difficulty in muon momentum measurement, and the tendency of muons to scatter in the target and thus blur the image. No direct information about the muon path traversing the medium under interrogation is available and some type of extrapolation is required for muon imaging. Current reconstruction algorithms rely on simple assumptions for muon path estimation through the imaged object. One commonly used assumption is the use of a straight-line path defined by the incoming muon direction [15] or a straight-line crossing PoCA point along incident direction [16]. Overall, conventional tomographic algorithms struggle when using oversimplified muon trajectories and the obtained images are of poor spatial resolution. For robust muon tomography, flexible path and efficient algorithms are needed to model the MCS process and accurately estimate the trajectory of a muon as it traverses an object.

Point of Closest Approach (PoCA) assumes that in the process of traversing an object, a muon experiences a single Coulomb scatter at the closest distance between the

incident and exiting trajectories. This point is also known as the PoCA point. The PoCA trajectory consists of two segments: (1) the segment connecting the point of muon incidence to the PoCA point and (2) the segment connecting the PoCA point and the point at which the muon exits said volume. Contrary to conventional use of a straight path for a muon, in the this work a curved path is first incorporated into muon computed tomography in order to improve image quality. This method assumes that a muon travels along the so-called PoCA trajectory within our defined volume. A dry cask with a fuel assembly missing was used as a model, and the Monte Carlo code GEANT4 [17] was used to describe the passage of muons through matter. This paper describes the expected performance of this method for imaging of said casks.

COSMIC RAY MUONS

Cosmic radiation, originating mainly from outside our solar system constantly bombards the upper layers of the Earth's atmosphere. A small amount penetrates the atmosphere, where it collides with the molecules of the atmosphere and creates extensive showers of secondary particles, including muons, that eventually reach sea-level. Cosmic ray muons are charged particles, 200 times heavier than the electron, generated naturally in the atmosphere. They rain down upon the earth at an approximate rate of 10,000 particles m^{-2} min^{-1} [18]. A particle shower is represented schematically in Fig. 1.

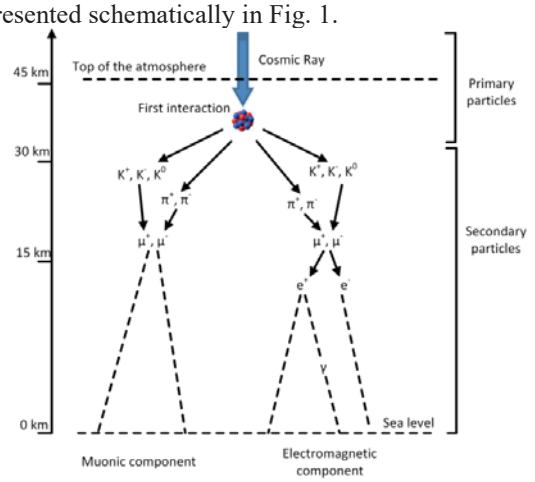

Fig. 1. Representation of a cosmic ray shower [19].

Cosmic muons passing through matter lose energy from inelastic collisions with the medium electrons and are deflected from nuclei by multiple Coulomb scattering (MCS). This deflection is the sum of all the small random contributions during a particle's path [20]. Different theories have been published of the multiple scattering of charged particles by matter. Of these, Moliere's theory, which remains analytical to the end and was later improved by Bethe [21], is in good agreement with most of experimental data. The complete calculation considers the loss of momentum of a muon as it traverses the medium:

$$\sigma_\theta^2 = A_0\left[1+0.038\ln\left(\int_{x_0}^{x_1}\frac{x}{X_0(x)}dx\right)\right]^2\int_{x_0}^{x_1}\frac{1}{\beta(x)^2p(x)^2}\frac{dx}{X_0(x)}. \quad (1)$$

Where A_0 is a constant derived from curve fitting. Assuming no energy loss and uniform material, Highland [22] suggests the following expression, currently adopted by the Particle Data Group:

$$\sigma_\theta^2 = \left(\frac{13.6\sqrt{2}\,MeV}{\beta cp}\sqrt{\frac{X}{X_0}}\left[1+0.038\ln\left(\frac{X}{X_0}\right)\right]\right)^2. \quad (2)$$

In Eqs. (1)-(2), p is the particle momentum in MeV/c, c is the speed of light, β is the ratio of particle speed to the speed of light, X is the thickness of the traversed medium, and X_0 is the radiation length - the characteristic quantity that describes the passage of muons through matter. In the present work, radiation length was calculated using Eq. (3) [23]:

$$\frac{1}{X_0} = 4\alpha r_e^2\frac{N_A}{A}\{Z^2[L_{rad}-f(Z)]+ZL'_{rad}\}, \quad (3)$$

where Z, A, r_e, N_A are the atomic number, atomic mass, Bohr radius and Avogadro's number, respectively and:

$$L_{rad} = \ln\left(184.15Z^{-1/3}\right), \quad (4)$$

$$L'_{rad} = \ln\left(1194Z^{-2/3}\right), \quad (5)$$

for materials relevant to sealed containers. The function $f(Z)$ is an infinite sum; but for elements up to uranium, it can be accurately represented by:

$$f(Z) = \alpha^2[(1+\alpha^2)^{-1}+0.20206-0.0369\alpha^2+0.0083\alpha^4-0.002\alpha^6]. \quad (6)$$

VALIDATION

To test the capability of our CT framework and muon tracing method to reconstruct the geometrical and material information of arbitrary objects, six cubes made of Al, Fe, Cu, Pb, W, and U were simulated using GEANT4. The cubes were placed between two pairs of position sensitive detectors. Parallel monoenergetic muons were generated. The muon source and detectors were rotated simultaneously 89 times at an azimuthal angle increment of 2° to generate 89 views. The pixel size was 1×1 cm^2. The configuration is shown on the left in Fig. 2. The scattering angles were registered for each muon and filtered back-projection (FBP) was used for reconstruction. The reconstructed image is shown on the right in Fig. 2. The

simulated and reconstructed image show very good agreement providing confidence in our capability to correctly model and reconstruct muon transport phenomena..

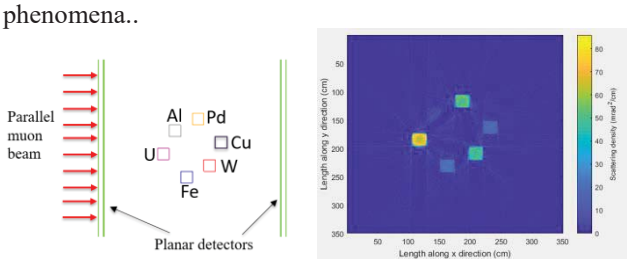

Fig. 2. Top-down view of configuration of six cubes, detectors and muon beam (on the left) and corresponding reconstructed image (on the right).

GEANT4 SIMULATIONS

The Monte Carlo code GENT4 was used to simulate a dry storage cask loaded with spent nuclear fuel, and two pairs of muon detectors placed on opposite sides. Polyenergetic-polydirectional cosmic ray muons were generated using a Muon Event Generator [19]. The simulated dry cask geometry is illustrated in Fig. 3. The dry cask was fully loaded with one fuel assembly missing from row 3. Two pairs of planar detectors, vertically offset by 100 cm, positioned along the sides of the dry cask were simulated. The separation between planes in each pair of detectors was 10 cm. The zenith angle was ~50° to increase the available muon flux which was ~20,000 muons/min.

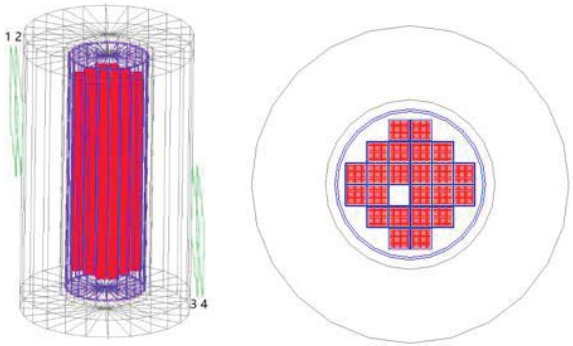

Fig. 3. Side (left) and top-down (right) views of the cask and detectors built in Geant4. An assembly has been removed from Row 3 (Row numbering starts from the left).

The detectors, each 350 cm wide by 150 cm high, were planes with perfect spatial and energy resolution. In our implementation, the cask containing the spent fuel assemblies was fixed, and the detectors rotated around it. The detectors were rotated at 2° increments to collect data from multiple views. Spent nuclear fuel emitted radiation was not simulated here. For muon i registered by four detectors with interaction point (x_{1i}, y_{1i}, z_{1i}) (x_{2i}, y_{2i}, z_{2i}), (x_{3i}, y_{3i}, z_{3i}) and (x_{4i}, y_{4i}, z_{4i}), the absolute incident horizontal direction angle φ_i was calculated:

$$\varphi_i = angle((x_{2i} - x_{1i}), 1i * (y_{2i} - y_{1i})) \,. \tag{7}$$

The scattering angles θ_i were calculated using:

$$\theta_{ix} = atan\left(\frac{x_{4i} - x_{3i}}{z_{4i} - z_{3i}}\right) - atan\left(\frac{x_{2i} - x_{1i}}{z_{2i} - z_{1i}}\right)$$
$$\theta_{iy} = atan\left(\frac{y_{4i} - y_{3i}}{z_{4i} - z_{3i}}\right) - atan\left(\frac{y_{2i} - y_{1i}}{z_{2i} - z_{1i}}\right) \tag{8}$$
$$\theta_i = \sqrt{\frac{\theta_{ix}{}^2 + \theta_{iy}{}^2}{2}}$$

Using each muon's momentum to correct for the influence of polyenergetic muons and the recorded path length to correct for the influence of different trajectories, the normalized scattering angle of a muon is:

$$\theta_i{}' = \frac{p_i}{p_0}\sqrt{\frac{D}{L_i}}\theta_i \,, \tag{9}$$

where p_0 is the nominal momentum chosen to be 3 Gev/c, p_i is the incident momentum of muon i, D is the horizontal distance between detectors 2 and 3 and L_i is the distance between (x_{2i}, y_{2i}, z_{2i}) and (x_{3i}, y_{3i}, z_{3i}). Finally, the registered incident muon spectrum was divided into one-degree-wide azimuthal bins according to their incident horizontal direction angles φ, separating the incident muons into 180 quasi-parallel groups.

IMAGE RECONSTRUCTION USING POCA TRAJECTORY

For muons in each quasi-parallel beam subset, the scattering angle is back-projected into each pixel crossed by its PoCA trajectory. After repeating this for all muon in current subset, the following steps took place: (i) calculate the variance of scattering angle in each pixel, (ii) take the summation of variance along the muon's incident horizontal direction and (iii) store it into detector bin hit by incident horizontal direction as shown in Fig. 4. Detector plan is rotated around dry cask center for 2*(j-1) degree for j^{th} quasi-parallel beam subset. In a FPB-based reconstruction, the information stored in each detector bin is simply back projected into the space domain along the muon's incident horizontal direction. For ART-based reconstruction, the average path length in each pixel is used for the system matrix.

In this work, the reconstruction was implemented using the ART algorithm. A total of N=89 projections of the scattering density were used. The object to be reconstructed is digitized into 100×100 pixels, and the

scattering density was expressed as a 100^2 dimensional vector. The iterative reconstruction process is stopped when the maximum iteration number is reached or when the difference in successive iterations is smaller than a given threshold.

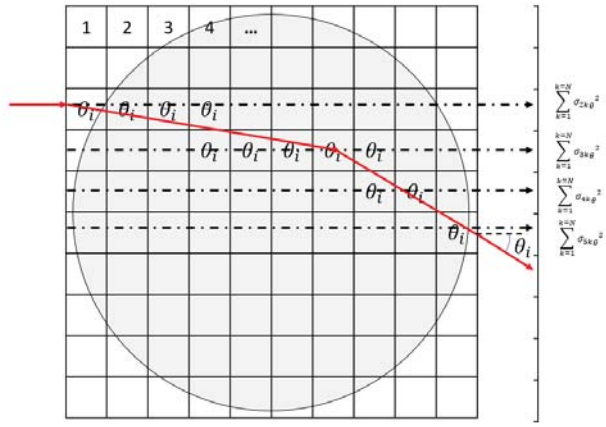

Fig. 4. Projection of the scattering angle along the PoCA trajectory and storing the variance into corresponding detector bins.

RESULTS AND DISCUSSION

Fig. 5 shows the reconstruction of the dry cask having a missing fuel assembly from row 3 using ART and the proposed muon tracing method. The reconstructions are shown with or without momentum information. If perfect momentum knowledge were available, the locations of the fuel assemblies may be expected to be identified—including the missing one. Further, the concrete overpack and the canister can be distinguished and separated from the fuel assemblies. When no momentum information is available, the simulation shows that location of the fuel assemblies can still be identified, including the missing one. Additionally, the concrete overpack can still be distinguished and separated from the fuel assemblies. However, the resolution is not expected to be good enough to identify the canister surrounding the fuel assemblies.

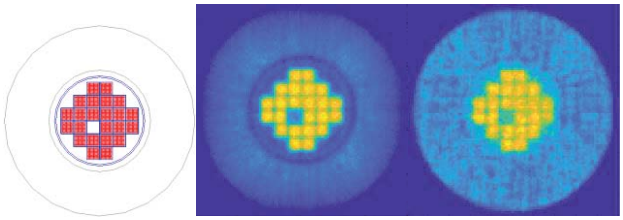

Fig. 5. ART reconstruction of a dry cask using PoCA trajectory. The simulated cask with one assembly missing is shown at the left. Simulated results are shown with perfect momentum measurement (center), and without momentum measurement (right).

To further test the detection capability of the proposed method, a dry cask with partial fuel assemblies missing from different locations was simulated in GEANT4. The reconstruction with and without momentum knowledge is shown in Fig. 6. One can expect the missing partial fuel assemblies to be identified even without momentum knowledge. This demonstrates our expectation about the improved capabilities of the method proposed herein.

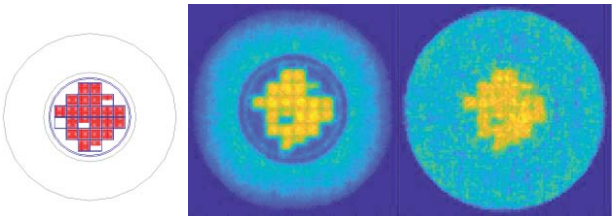

Fig. 6. ART reconstruction of a dry cask using the PoCA trajectory. The simulated cask with multiple half fuel assemblies missing is shown at the left. Simulated results are shown with perfect momentum measurement (center) and without momentum measurement (right).

ACKNOWLEDGMENTS

This research was performed using funding received from the DOE Office of Nuclear Energy's Nuclear Energy University Programs under contract DE-NE0008292. Research was partially sponsored by the Laboratory Directed Research and Development Program of Oak Ridge National Laboratory, managed by UT-Battelle, LLC, for the US Department of Energy.

REFERENCES

1. D. STEPHEN et al. "Aligning Technology, Policy and Culture to Enhance Nuclear Security: A Comparative Analysis of Nigeria and the US." *International Journal of Nuclear Security* 3.1 (2017): 7.
2. K. BOROZDIN et al., "Radiographic Imaging with Cosmic Ray Muons," *Nature*, **422**, 22 (2003).
3. K. BOROZDIN et al., "Cosmic Ray Radiography of the Damaged Cores of the Fukushima Reactors," Phys. Rev. Let., 109 152501 (2012).
4. L. J. SCHULTZ, "Cosmic Ray Muon Radiography," PhD dissertation, Portland State University (2003).
5. S. CHATZIDAKIS et al., "Interaction of Cosmic Ray Muons with Spent Nuclear Fuel Dry Casks and Determination of Lower Detection Limit," *Nucl. Instr. Methods Phys. Res. A*, **828**, 37–45 (2016).
6. V. ANGHEL et al., "A Plastic Scintillator-based Muon Tomography System with an Integrated Muon Spectrometer," *Nucl. Instrum. Methods, Phys. Res. A*, **798**, 12–23 (Oct. 2015).
7. S. PESENTE et al., "First Results on Material Identification and Imaging with a Large-volume Muon

Tomography Prototype," *Nucl. Instrum. Methods, Phys. Res. A*, **604**(3), 738–746 (2009).
8. P. BAESSO et al., "Toward a RPC Based Muon Tomography System for Cargo Containers," *J. Instrum.*, **9**, C10041 (Oct. 2014).
9. E. ASTROM et al., "Precision Measurements of Linear Scattering Density Using Muon Tomography," *J. Instrum*., **11**, P07010 (Jul. 2016).
10. S. CHATZIDAKIS et al., "Analysis of Spent Nuclear Fuel Imaging Using Multiple Coulomb Scattering of Cosmic Muons," *IEEE Trans. Nuc. Sci*., **63**, 2866 (2016).
11. J. M. DURHAM et al., "Cosmic Ray Muon Imaging of Spent Nuclear Fuel in Dry Storage Casks," *J. Nucl. Mater. Manage*., **44**, 3 (2016).
12. S. CHATZIDAKIS and L. H. TSOUKALAS, "Theoretical Investigation of Spent Nuclear Fuel Monitoring Using Cosmic Ray Muons," *International Congress on Advances in Nuclear Power Plants (ICAPP 2016)*, San Francisco, April 17–20, 2016.
13. Z. LIU et al., "Detection of Missing Assemblies and Estimation of the Scattering Densities in a VSC-24 Dry Storage Cask with Cosmic-Ray-Muon-Based Computed Tomography," *J. Nucl. Mater. Manage*., **45**, 12 (2017).
14. S. CHATZIDAKIS, C.K. CHOI, and L. H. TSOUKALAS, "Investigation of Imaging Spent Nuclear Fuel Dry Casks Using Cosmic Ray Muons," *Trans. Am. Nucl. Soc.*, **114**, 152–155 (2016).
15. D. POULSON et al. "Cosmic Ray Muon Computed Tomography of Spent Nuclear Fuel in Dry Storage Casks," *Nucl. Instr. Meth. Phys. Res. A*, **842**, 48–53 (2017).
16. Z. LIU et al., "Characteristics of Muon Computed Tomography of Used Fuel Casks Using Algebraic Reconstruction," *IEEE Nucl. Sc. Symp. Conf. Record* (2017).
17. S. AGOSTINELLI et al., "GEANT4—A Simulation Toolkit," *Nucl. Instr. Meth. Phys. Res. A*, **506**, 250–303 (2003).
18. K. HAGIWARA, "Review of Particle Physics," *Phys. Rev. D*, **66**(1), 010001 (2002).
19. S. CHATZIDAKIS et al., "Developing a Cosmic Ray Muon Sampling Capability for Muon Tomography and Monitoring Applications," *Nucl. Instr. Meth. Phys. Res. A*, **804**, 33–42 (2015).
20. S. CHATZIDAKIS et al., "Exploring the Use of Muon Momentum for Detection of Nuclear Material Within Shielded Spent Nuclear Fuel Dry Casks," *Trans. Am. Nucl. Soc.*, **116**, 190–193 (2017).
21. H. A. BETHE, "Moliere's Theory of Multiple Scattering," *Physical Review*, **89**, 1256 (1953).
22. V. L. HIGHLAND, "Some Practical Remarks on Multiple Scattering," *Nucl. Inst. Meth.,* **129**, 497–199 (1975).
23. A. A. M. MUSTAFA & D. F. JACKSON, "Small-angle Multiple Scattering and Spatial Resolution in Charged Particle Tomography," *Phys. Med. Biol.*, **26**, 461–472 (1981).